

Geometric Mixing

Julyan H. E. Cartwright,¹ Emmanuelle Gouillart,² Nicolas Piro,³ Oreste Piro,⁴ and Idan Tuval⁵

¹*Instituto Andaluz de Ciencias de la Tierra, CSIC–Universidad de Granada, Campus Fuentenueva, E-18071 Granada, Spain*

²*Surface du Verre et Interfaces, UMR 125 CNRS/Saint-Gobain, 93303 Aubervilliers, France*

³*École Polytechnique Fédérale de Lausanne, CH-1015 Lausanne, Switzerland*

⁴*Departament de Física, Universitat de les Illes Balears, E-07071 Palma de Mallorca, Spain*

⁵*Department of Global Change Research, Mediterranean Institute for Advanced Studies (CSIC-UIB), E-07190 Esporles, Spain*

Mixing fluid in a container at low Reynolds number — in an inertialess environment — is not a trivial task. Reciprocating motions merely lead to cycles of mixing and unmixing, so continuous rotation, as used in many technological applications, would appear to be necessary. However, there is another solution: movement of the walls in a cyclical fashion to introduce a geometric phase that avoids unmixing. We show using journal-bearing flow as a model that such geometric mixing is a general tool for using deformable boundaries that return to the same position to mix fluid at low Reynolds number.

PACS numbers: 05.45.-a, 47.51.+a, 47.52.+j

How may fluid be mixed at low Reynolds number? Such mixing is normally performed with a stirrer, a rotating device within the container that produces a complex, chaotic flow. Alternatively, in the absence of a stirrer, rotation of the container walls themselves can perform the mixing, as occurs in a cement mixer. At the lowest Reynolds numbers, under what is known as creeping flow conditions, fluid inertia is negligible, fluid flow is reversible, and an inversion of the movement of the stirrer or the walls leads — up to perturbations owing to particle diffusion — to unmixing, as Taylor [1] and Heller [2] demonstrated. This would seem to preclude the use of reciprocating motion to stir fluid at low Reynolds numbers; it would appear to lead to perpetual cycles of mixing and unmixing. The solution to this conundrum involves a geometric phase induced by a cyclic variation of the boundary shape. A geometric phase [3] is an example of anholonomy: the failure of system variables to return to their original values after a closed circuit in the parameters. In this Letter we propose what we term geometric mixing: the use of the geometric phase introduced by the deformable boundaries of a container as a tool for fluid mixing at low Reynolds number. We note that since a flow produced by a reciprocal cycle of the boundaries induces an identity map for the positions of each fluid element at successive cycles, the problem of mixing by nonreciprocal ones is closely related to the class of dynamical systems constituted by perturbations of the identity. The structure of chaos in this class of dynamics has been greatly overlooked in the literature, and the present research opens a new avenue to the understanding of this associated problem. To exemplify how this process leads to efficient mixing, we use the well-known two-dimensional mixer based on the journal bearing flow but subject to a much-less-studied rotation protocol that satisfies geometrical constraints. We lastly propose that such a geometric phase — the “belly phase” [4] — may be found in the stomach.

Taylor [1] and Heller [2] used the Couette flow of an incompressible fluid contained between two concentric cylinders to demonstrate fluid unmixing due to the time reversibility of the Stokes regime. They showed that after rotating the cylinders

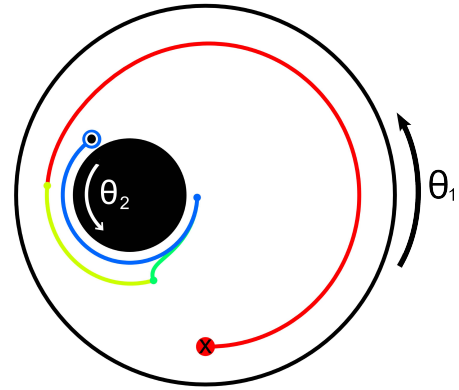


FIG. 1: The journal bearing flow with cylinder radii $R_1 = 1.0$, $R_2 = 0.3$ and eccentricity $\varepsilon = 0.4$, taken around a square closed parameter loop with $\theta_1 = \theta_2 \equiv \theta = 2\pi$ radians. The four segments of the loop are plotted in different colours (red, yellow, green, blue) to enable their contributions to the particle motion to be seen. A trajectory initially at $(0.0, -0.8)$ is shown.

through a certain angle, it is possible to arrive back at the initial state — to unmix the flow — by reversing this rotation through the same angle with the opposite sign, even when the angle is large enough that a blob of dye placed in the fluid has been apparently well mixed. Considering as parameters in this device the positions of the outer and inner cylindrical walls of the container specified respectively with the angles θ_1 and θ_2 from a given starting point, a geometric phase might arise from driving this system around a loop in the parameter space. In general, if one takes a system through a parameter loop, one obtains as a result three phases: a dynamic phase, a nonadiabatic phase, and a geometric phase. If one then traverses the same loop in the opposite direction, the dynamic phase accumulates as before, while the geometric phase is reversed in sign. To get rid of the nonadiabatic phase too one must travel slowly around the loop. However, in a fluid system in the Stokes regime, like ours, the motion is by definition always adiabatic and only associated with the change in

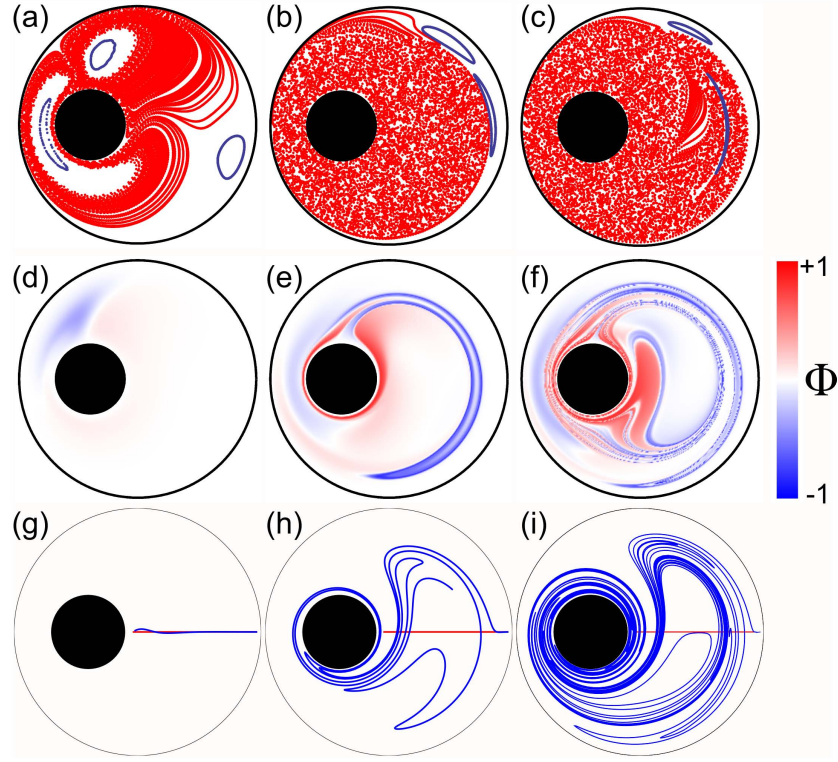


FIG. 2: (a–c) Poincaré maps demonstrate geometric mixing for the journal–bearing flow for the same cylinder radii and eccentricity as in Fig. 1. Chaotic trajectories are marked in red while regular ones in blue. 10 000 iterations of the parameter loop are shown for: (a) $\theta = \pi/2$ radians; (b) $\theta = 2\pi$ and (c) $\theta = 4\pi$. (d–f) The geometric phase across the domain for the same parameters; the color scale denoting the phase at a given point is given by the intensity of red, positive and blue, negative. (g–i) The evolution of a line segment (initial segments in red) across the widest gap between the cylinders after one cycle for the same parameters (final segments in blue).

the parameters: the positions of the cylinders. Therefore, any resulting phase would be a geometric phase. In the Heller–Taylor demonstration the parameter loop is very simple: θ_1 first increases a certain amount and then decreases the same amount while θ_2 remains fixed. This loop encloses no area, and reversibility ensures that the phase is zero. More complex *zero-area* loops can be constructed by combining in succession arbitrary pairs of reciprocal rotations of both cylinders, and they also lead to a null phase. We shall call these constructs *reciprocal cycles*. In order to consider less trivial loops, we first notice that the parameter space is homotopic to a 2-torus. Loops on such a space can be classified according to the number of complete turns that both parameters accumulate along the loop. Note also that a relative rotation of 2π between the walls brings the container to the original configuration except for a global rotation. However, with the application to peristaltic mixing in view, we consider only the class of type-0 or *contractible* (to a point) loops. These loops do not imply any net relative displacement of the walls.

All zero-area reciprocal loops are contractible, but there are many more enclosing a finite area. To obtain a finite-area non-reciprocal contractible loop we can, for instance, rotate first one cylinder, then the other, then reverse the first, and finally reverse the other. However, for concentric cylinders

the streamlines are concentric circles; if we move one of the cylinders by angle θ , a tracer particle will move along a circle an angle $f_r(\theta)$ that only depends on θ . Then it is obvious that the cumulative effect of moving one cylinder θ_1 , then the other θ_2 , then the first $-\theta_1$, and the second $-\theta_2$, is to return the particle to its original position: there is no geometric phase, and unmixing still occurs. But if we modify the Heller–Taylor setup and offset the inner cylinder, we arrive at what is known as journal–bearing flow. On introducing an eccentricity ε between the cylinders, this flow has a radial component. In the creeping-flow limit, the Navier–Stokes equations for the journal–bearing flow reduce to a linear biharmonic one, $\nabla^4 \psi = 0$, and we may model this system utilizing an analytical solution of the stream function in bipolar coordinates [5–7]. If we now perform a parameter loop by the sequence of rotations detailed above, we arrive back at our starting point from the point of view of the positions of the two cylinders, so it is, perhaps, surprising that the fluid inside does not return to its initial state. We illustrate the presence of this geometric phase in Fig. 1 in which an example of the trajectory of a fluid particle is shown as the walls are driven through a nonreciprocal contractible loop. Journal–bearing flow has been studied in the past [8–11], but never with contractible loops so that this geometric effect was never emphasized. A fluid particle that

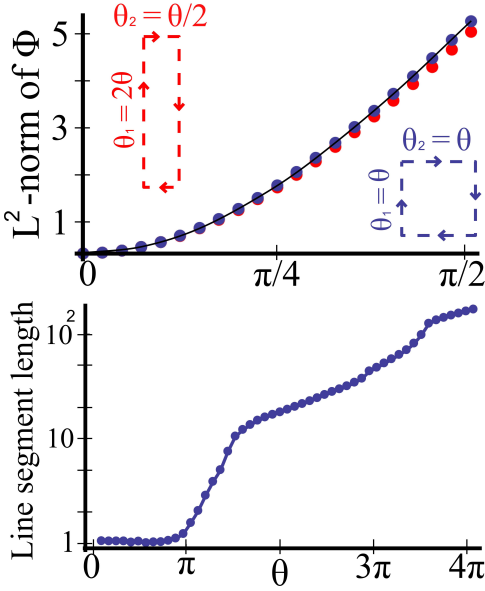


FIG. 3: (a) The L^2 -norm of the Φ field grows quadratically with θ for loops with small area. Two distinct loops with equal area are shown. (b) The final length of a line segment as shown in Figure 2(g–i) plotted after one cycle for flows with different rotation angles θ .

at the beginning of the loop is in a position (x, y) , reaches, at the end of the same loop, a unique corresponding point (x', y') which is a one-to-one function $(x', y') = \mathbf{T}[(x, y)]$ of the initial one. For homogeneous fluids, \mathbf{T} must also be continuous and differentiable, whereas incompressibility implies that \mathbf{T} preserves the area of any domain of points. In other words, incompressible flow implies Hamiltonian dynamics for the fluid particles, and the map that this dynamics induces in one loop is area preserving. For contractible zero-area loops the map is simply the identity; each particle ends in the position in which it started. Hence, a finite-area loop induces, in general, a finite deviation from the identity map and a characteristic value of the geometrical phase gives an estimate for the extent of this deviation. Since generically the geometric phase increases with the area of the loop (see Fig. 3(a)), for small loops the map is a small perturbation away from the identity whereas loops of greater area induce larger deviations.

Let us now consider the long-term fluid dynamics elicited by a repeated realization of the same contractible non-reciprocal loop that induces a given map. The dynamics is described by the repeated iteration of this map that acts as the stroboscopic map of the time-periodic Hamiltonian system constituted by the incompressible flow periodically driven by the motion of the walls. For small loops, the map is a small perturbation of the identity that can be thought of as the implementation of the Euler algorithm for a putative continuous time dynamical system defined by this perturbation. Therefore, in 2D we expect that the iterations of the map will closely lie on the trajectories of this 2D continuous system which is integrable. Therefore, fluid particles will mix very slowly in

space. This is nicely illustrated in Fig. 2(a), where even for a square loop formed with values as large as $\theta = \pi/2$ the position of the fluid particles after successive loops smoothly shift along the closed curves that are the trajectories of the referred continuous dynamics. The trajectories are composed of segments that nearly follow the integrable trajectories of a 2D flow (approximated as an Euler map) until it reaches the region of large phase, where chaos and heteroclinic tangles occur. There the particle jumps into another quasi-integrable trajectory, until it again reaches the region of large phase. In typical Hamiltonian chaos (the standard map, for example) the map is not a perturbation of the identity but a perturbation of a linear shear ($I' = I$, $\varphi' = \varphi + I'$) for which reason this behavior is not normally seen.

As the geometric phase and the corresponding perturbation from the identity map increase, the former argument begins to fail [12]. A more chaotic 2D-area preserving map emerges and with it the corresponding space-filling fully chaotic trajectories. The KAM islands typically become smaller and smaller as the characteristic values of geometric phase increase. As we see in Fig. 2(b) for $\theta = 2\pi$ radians, and even more so in 2(c), $\theta = 4\pi$ radians, after 10 000 cycles the fluid particle has covered most of the area available to it between the two cylinders. This is fluid mixing induced entirely by a geometric phase; we may call it geometric mixing. Geometric mixing therefore creates chaotic advection [10], as does the classical journal-bearing protocol.

In Fig. 2(d–f) we show the corresponding distributions of the geometric phase over the domain. The value of the geometric phase at a given initial position, obtained in terms of the final angle minus the initial angle in bipolar coordinates after one iteration, $\Phi = \xi_f - \xi_i$, is plotted on a color scale of intensities of red (positive) and blue (negative). Note that the phase goes to zero at the walls, as it must, but varies strongly across the domain. In particular, for parameters of $\theta = 2\pi$ radians (Fig. 2(e)), we see the development of a tongue of high values of the geometric phase in one sense interpenetrating a region of high values of the phase in the opposite sense. The trajectory plotted in Fig. 1 shows the origin of the tongue; fluid particles that are advected to the vicinity of the inner cylinder by the first θ_1 step are then advected to a significantly different value of r by the inner cylinder. As a result, the fluid particle is located on a completely different streamline from the first step when the outer cylinder starts rotating backwards. As may be expected, for smaller parameter values this tongue is absent (Fig. 2(d)). At even higher values of θ , on the other hand, (Fig. 2(f)) the tongue wraps twice round in a highly complex fashion. In Fig. 2(g–i) we show by plotting the evolution of a line of initial conditions how the geometric phase is related with the dynamical structures in the flow. Figure 2(g), for $\theta = \pi/2$ radians, shows that when this tongue is absent, the line segment hardly evolves; the flow is almost reversible. The line segments for Fig. 2(h), and (i), for $\theta = 2\pi$ and 4π radians, on the other hand, show a great deal of stretching induced by this tongue of large geometric phase. To demonstrate this effect of the geometric phase on the flow

in more detail, in Fig. 3(b) we plot the length of the line segment after a single cycle against the rotation angle. A notable aspect of this plot is that it displays plateaux separated by periods of rapid growth. A comparison with Fig. 2(d–f) shows that it is the penetration of the tongue of large values of the geometric phase across this line segment that induces stretching. The tongue penetrates a first time before $\theta = 2\pi$, and then a second time before $\theta = 4\pi$, so producing two jumps; between these jumps the evolution of the line segment is much slower. For a given energy cost, which scales with the total unsigned displacement of the walls, geometric mixing is therefore more efficient for a large value of θ .

The journal-bearing flow is just one example of a class of flows that display geometric mixing. Another flow that was studied early on in chaotic advection is the rectangular cavity flow, in which one or more of the walls of a fluid filled rectangular container can move, being set up as conveyor belts [10, 13]. In the same way as in the journal-bearing case one can introduce a geometric phase by returning all the walls to their initial positions after a loop in the parameters. More generally, one can conceive of flows in which the walls do not move as rigid bodies, but instead can deform longitudinally and/or tangentially.

The stomach is a biological instance of such a cavity flow [14, 15]. In the stomach food and drink are mixed to form a homogeneous fluid termed chyme, which is then digested by the intestines. Gastric mixing is produced by what is called peristalsis: by the stomach walls moving in a rhythmic fashion. In mathematical terms, the shape of the stomach walls undergoes a closed cycle in the space of shapes during each peristalsis cycle. Obviously only shape cycles that do not require a cumulative net displacement between any two sections of the stomach can be considered. How then is this peristaltic movement of the stomach walls able to produce mixing, especially in animals in which the stomach dimensions are such that fluid inertia of the stomach contents is negligible?

The human stomach is a strong muscular receptacle between the oesophagus and the small intestine. It is not just a storage chamber for food, but also a mixer where the chyme is prepared. The human stomach has a volume L^3 of some 330 mL, while the viscosity μ of the chyme is of order 1 Pa s, its density is $\rho \approx 10^3 \text{ kg m}^{-3}$, and the maximum flow velocities V observed are in the range $2.5\text{--}7.5 \text{ mm s}^{-1}$ [14]. From these data we may estimate the Reynolds number $Re = \rho VL/\mu$ to lie in the range 0.2–0.5. Thus we may conclude that in the human stomach fluid inertia has only limited importance, and in any smaller animal it will be inappreciable.

The gastric mixing is brought about by peristaltic waves — transverse traveling waves of contraction — that propagate along the stomach walls at some 2.5 mm s^{-1} . They are initiated approximately every 20 s, and take some 60 s to pass the length of the stomach, so 2–3 waves are present at one time, while on average the stomach width as the wave passes is 0.6 times its normal width [14, 15]. We thus have their velocity $c = 2.5 \text{ mm s}^{-1}$, frequency $f = 0.05 \text{ Hz}$, and thence wavelength $\lambda = c/f = 5 \text{ cm}$, and their amplitude

$a = 1/2 \times 0.6L \approx 2 \text{ cm}$. These waves force the stomach through a nonreciprocal loop in the space of shapes, as a result of which geometric mixing is expected. One can give a rough estimate of the size of the expected geometric phase by taking advantage of results obtained for another geometric phase problem: that of low-Reynolds-number microorganisms swimming. Many bacteria swim by deforming their bodies in the same way as the peristaltic waves of the stomach and their speed has been well estimated by modeling such deformations as plane waves [16]. Similar calculations for the stomach render the flow velocity induced by the peristaltic waves $V = \pi c(a/\lambda)^2$, which comes out at approximately 1 mm s^{-1} , from where a displacement of about 6 cm per peristaltic cycle is expected or, considering a circular stomach of radius L , a geometric phase of the order of 2 radians.

The importance of the geometric mixing in the stomach may be appreciated by reference to instances in which it is disrupted. The stomach is like the heart, with electrical activity from a pacemaker region stimulating oscillations; in this case being traveling waves of peristalsis. If this system is not working correctly, there can be gastroparesis or gastric fibrillation [17, 18], in which the peristaltic waves become disordered. In our terms, there is poor mixing or no mixing in gastroparesis because there is not a loop around the space of forms, so no geometric phase, and instead random peristaltic waves induce only mixing and unmixing.

We acknowledge the financial support of the grant FIS2010-22322-C02-01/02 from MICINN and from the “subprograma Ramon y Cajal” (I.T.).

-
- [1] G. I. Taylor, *Low Reynolds Number Flow* (Educational Services Incorporated, 1960), (16 mm film).
 - [2] J. P. Heller, *Am. J. Phys.* **28**, 348 (1960).
 - [3] A. Shapere and F. Wilczek, eds., *Geometric Phases in Physics* (World Scientific, 1989).
 - [4] We are indebted to Michael Berry for this coinage.
 - [5] G. B. Jeffery, *Proc. Roy. Soc. Lond. A* **101**, 169 (1922).
 - [6] B. Y. Ballal and R. S. Rivlin, *Arch. Ration. Mech. Anal.* **62**, 237 (1976).
 - [7] M. D. Finn and S. M. Cox, *J. Eng. Math.* **41**, 75 (2001).
 - [8] H. Aref and S. Balachandar, *Phys. Fluids* **29**, 3515 (1986).
 - [9] Chaiken et al., *Proc. Roy. Soc. Lond.* **408**, 165 (1986).
 - [10] J. M. Ottino, *The Kinematics of Mixing: Stretching, Chaos, and Transport* (Cambridge University Press, 1989).
 - [11] M. Tabor, *Chaos and integrability in nonlinear dynamics: an introduction* (Wiley, 1989).
 - [12] J. H. E. Cartwright and O. Piro, *Int. J. Bifurcation and Chaos* **2**, 427 (1992).
 - [13] Ottino et al., *Nature* **333**, 419 (1988).
 - [14] Pal et al., *Proc. Roy. Soc. Lond. B* **271**, 2587 (2004).
 - [15] K. Schulze, *Neurogastroenterol. Motil.* **18**, 172 (2006).
 - [16] J. Koiller, K. Ehlers, and R. Montgomery, *J. Nonlinear Sci.* **6**, 507 (1996).
 - [17] Lin et al., *Digestive Diseases and Sciences* **48**, 837 (2003).
 - [18] Rinaldi et al., *Nutritional Therapy and Metabolism* **27**, 134 (2009).